International Soil and Water Conservation Research 7 (2019) 167–175

Contents lists available at ScienceDirect

International Soil and Water Conservation Research

journal homepage: www.elsevier.com/locate/iswcr

Original Research Article

Dynamic study of infiltration rate for soils with varying degrees of degradation by water erosion

Yujie Wei, Xinliang Wu, Jinwen Xia, Rubing Zeng, Chongfa Cai *, Tianwei Wang

Key Laboratory of Arable Land Conservation (Middle and Lower Reaches of Yangtze River) of the Ministry of Agriculture, Soil and Water Conservation Research Centre, College of Resources and Environment, Huazhong Agricultural University, Wuhan 430070, China

ARTICLE INFO

Article history:
Received 4 September 2018
Received in revised form
27 December 2018
Accepted 28 December 2018

Keywords:
Soil infiltration
Rainfall simulation
Erosional degradation
Soil texture
Water erosion

ABSTRACT

Ultisols, widely distributed in tropical and subtropical areas of south China, are suffering from serious water erosion, however, slope hydrological process for Ultisols under different erosional degradation levels in field condition has been scarcely investigated. Field rainfall simulation at two rainfall intensities (120 and 60 mm/h) were performed on pre-wetted Ultisols with four erosion degrees (non, moderate, severe and very-severe), and the hydrological processes of these soils were determined. The variation of soil infiltration was contributed by the interaction of erosion degree and rainfall intensity ($p < 0.05$). In most cases, time to incipient runoff, the decay coefficient, steady state infiltration rate, and their variability were larger at the high rainfall intensity, accelerating by the increasing erosion severity. Despite rainfall intensity, the infiltration process of Ultisols was also significantly influenced by mean weight diameter of aggregates at the field moisture content, soil organic carbon and particle size distribution ($R^2 > 30\%$, $p < 0.05$). The temporal erodibility of surface soil and soil detachment rate were significantly and negatively correlated with infiltration rate ($r < -0.32$, $p < 0.05$), but less significant correlation was observed between sediment concentration and infiltration rate for most soils, especially at the high rainfall intensity. The variation of surface texture and soil compactness generated by erosion degradation was the intrinsic predominant factors for the change of infiltration process of Ultisols. The obtained results will facilitate the understanding of hydrological process for degraded lands, and provide useful knowledge in managing crop irrigation and soil erosion.

© 2019 International Research and Training Center on Erosion and Sedimentation and China Water and Power Press. Production and Hosting by Elsevier B.V. This is an open access article under the CC BY-NC-ND license (http://creativecommons.org/licenses/by-nc-nd/4.0/).

1. Introduction

Rainfall infiltration is a process that water runs into the soil and leads to an increased total moisture content, contributing to the variation of water partitioning and hydrologic response, and changes the development and recurrence frequency of erosion process (Lu, Zheng, Li, Bian, & An, 2016; Shakesby, Doerr, & Walsh, 2000; Walker, Walter, & Parlange, 2007). To better understand the hydrological and erosion mechanism in tropical and subtropical areas, rainfall infiltration pattern and process should gain more consideration in those regions where precipitation is the dominant source for soil erosion.

The process of rainfall infiltration is controlled by several factors, including geomorphology, rainfall or climatic properties, surface roughness, soil porosity or density, organic carbon content, size and stability level of the aggregates, and soil hydraulic properties (Mohamadi & Kavian, 2015; Morbidelli, Saltalippi, Flammini, & Govindaraju, 2018). These factors consequently interfere on runoff. Prior research generally confirmed that land cover significantly affects infiltration, reducing the direct impact of raindrops on the soil (Almeida et al., 2018). Soil surface roughness, porosity and infiltration decrease due to the limited plant canopy or residue cover for bare soils, causing the increase of runoff and intensification of the erosion process. Widely accepted that, the formation of surface crust is the predominant process influencing soil infiltration during the rainfall, especially for bare lands (e.g., Assouline, 2004; Durán Zuazo & Rodríguez Pleguezuelo, 2008; Le Bissonnais et al., 2005; Podwojewski et al., 2011). Soils with low aggregate stability but high dispersivity form a surface crust much more readily, resulting in the development of a dense, thick and less permeable surface structure (Le Bissonnais, 1996; Rodrigo Comino et al., 2016).

A consensus on an explanation for the influence of rainfall intensity on infiltration rate could be hardly obtained in literatures,

* Corresponding author.
E-mail address: hzaucfcai@163.com (C. Cai).

Peer review under responsibility of International Research and Training Center on Erosion and Sedimentation and China Water and Power Press.

https://doi.org/10.1016/j.iswcr.2018.12.005

2095-6339/© 2019 International Research and Training Center on Erosion and Sedimentation and China Water and Power Press. Production and Hosting by Elsevier B.V. This is an open access article under the CC BY-NC-ND license (http://creativecommons.org/licenses/by-nc-nd/4.0/).

and reversed results have been reported in prior publications (e.g., Assouline & Ben-Hur, 2006; Liu, Lei, Zhao, & Yuan, 2011). High rainfall intensity accelerates the dispersion and breakdown of aggregate, facilitating the formation of surface seal. However, an increase in rain intensity lead to a higher transportability of flow, enhancing the mobility the detached particles carried away out of the test area. Briefly, the variation of land surface condition generating the change of infiltration pattern and process should be controlled by the comprehensive effects of rainfall character and the stability of soil structure.

Water erosion, as the most predominant erosion type in tropic and sub-tropic areas, encompasses infiltration, percolation and retention under rainfall (Bossio, Geheb, & Critchley, 2010). Bare lands resulted from erosional degradation are widely distributed around the world, creating severe limitations to the sustainability of natural ecosystems and agricultural activities (García-Ruiz, Beguería, Lana-Renault, Nadal-Romero, & Cerdà, 2017; Gonzalez, 2018; Podwojewski et al., 2011). Land degradation results in the reduction of water productivity, availability, quality and storage at field and landscape scales (Lal, 2001), and caused the deterioration of soil physical, chemical and hydrological process (Bhan, 2013; Le Bissonnais et al., 2005). The reduction of water productivity, availability, quality and storage, the deterioration of soil physical, chemical and hydrological process generated by land degradation are the chronic problems particular for the tropic and sub-tropic areas. Soil thickness declines in various degrees and even has the parent material horizons exposed during the intensification of soil erosion process (Zhang, Yang, & Zepp, 2004). It is traditionally recognized that pedogenic differentiation, including aggregate stability, porosity, density and organic matter et al., leads to the heterogeneity of soil properties in different horizons (e.g., Rejman, Turski, & Paluszek, 1998; Wu, Cai, Wang, Wei, & Wang, 2016). The variability of soil properties resulted from degradation would definitely in turn alters the soil infiltration process (e.g., Assouline, 2004; Carmi & Berliner, 2008; Malvar, Martins, Nunes, Robichaud, & Keizer, 2013).

Most of the existing studies about the correlation between infiltration, soil loss, and surface condition have been performed on small plots with rainfall simulation in laboratory (Cerdà, 1999; Huang, Wu, & Zhao, 2013), but crust formation generated by raindrop impact under natural field conditions is significantly different from crusting in disturbed soil samples in laboratory (Abudi, Carmi, & Berliner, 2012). Ultisols, as the representative quaternary red clay soils in subtropical and tropical regions of central-south China, suffer from serious water erosion. However, few research has been conducted to investigate the infiltration process of Ultisols under different erosion-induced degradation degrees, particular at the field condition.

In accordance with the aforementioned background, this study aims at (i) characterizing the temporal variation of rainfall infiltration process under various erosion-induced degradation degrees at two contrasting rainfall intensities, and (ii) identifying the key physicochemical parameters that account for the dynamic infiltration response indexes. To end this, field plot rainfall simulation experiments were conducted on bare Ultisols with four erosion degrees (non, moderately, severely and very severely eroded) pursuant to the outcrop of eluvium, illuvium and parent material horizons. The obtained results will supplement the knowledge of soil hydrological process of the degraded lands in water erosion dominated regions.

2. Materials and methods

2.1. Experimental sites and soils

Ultisols, derived from quaternary red clay, are the representative soils in subtropical and tropical regions, which occupies 16% of the total areas in China (Fig. S1) (Gao, Li, & Zhou, 1998). East Asian Monsoon climate with the rainy season coinciding with high temperature dominates the climate in these regions. Hilly land with a relative elevation of 10–60 m and a gentle slope ($< 15°$) is the main farmland resource in these areas, and the intensive cultivation makes the soils here are prone to erosion. Water erosion has been a great threat to land productivity and environment protection.

In accordance with the principle of typicality of soil types and accessibility of field rainfall simulation, Ultisols were selected from the north of Changsha city (28°30′N, 112°54′E), Hunan Province, China (Fig. 1-a). The mean annual precipitation and temperature in this area is 1422 mm and 17 °C, respectively. Field plots suffering from different water erosion degrees were selected according to the outcrop the pedogenic horizons (Rejman, Turski, & Paluszek, 1998): soil profile with the intact eluvial horizon (A) was in a non-erosion degree (E0); soil profile with the outcrop of illuvial horizons, B1 and B2, was in the moderate (E1) and severe (E2) erosion degree, respectively; soil profile with the outcrop of parent material horizon (C) was very severely eroded (E3) (Fig. S2). Characteristics of each horizon were summarized in Table 1. Before the installment of field plot, top soil layers (about 1–3 cm thickness) with roots and organic residues were removed to avoid the interference of vegetation impacts. The basic information of Ultisols with different erosion degrees was summarized in Table 2.

2.2. Measurement of rainfall infiltration

Soil infiltration generated by rainfall was determined by field plot rainfall simulation experiments. Field plots for rainfall simulation were equally in an area of 2.40 m^2 (length 3.00 m × width 0.80 m) and at a slope of 10° (the representative slope gradient in this region) (Fig. 1-b). Two repetitions were performed due to the intensive labor and the capture area of the portable rainfall simulator. Big clods (< 3 cm) in the surface layer (< 5 cm) were crushed to simulate the cropland condition. Besides, the plots were presaturated for the consistency of the antecedent water condition, and the raindrop energy was retard with a 2-mm wire screen suspended 0.10 m above the soil surface. The rainfall experiment was conducted after 12 h of the runoff generation.

Rainfall simulator with a SPRACO cone jet nozzle was installed at a height of 5.0 m above the center of the plots to obtained a natural raindrop energy when rain drops approached soil surface (Luk, Abrahams, & Parsons, 1986). In accordance with the representative and common rainstorms in study area, two rainfall intensities (60 and 120 mm/h) were designed. Rainfall simulation was continued for 1 h after runoff initiation. Runoff and sediment were collected at 3-min intervals after runoff generation for measurement of runoff volume (L) and soil loss (g). Infiltration was determined by difference from runoff and rainfall intensity.

Infiltration rate (f) was calculated by difference between rainfall intensity and runoff rate. The infiltration curves were fitted by the Horton (1941):

$$f = \begin{cases} f_0 & T < T_r \\ f_c + \left(f_0 - f_c\right)e^{-k(T-T_r)} & T \geq T_r \end{cases} \quad (1)$$

where, f_0 and f_c are the initial and steady state infiltration rate, respectively (mm/min); k is the Horton's decay coefficient; T_r is the time to incipient runoff (min); T is the rainfall duration (min).

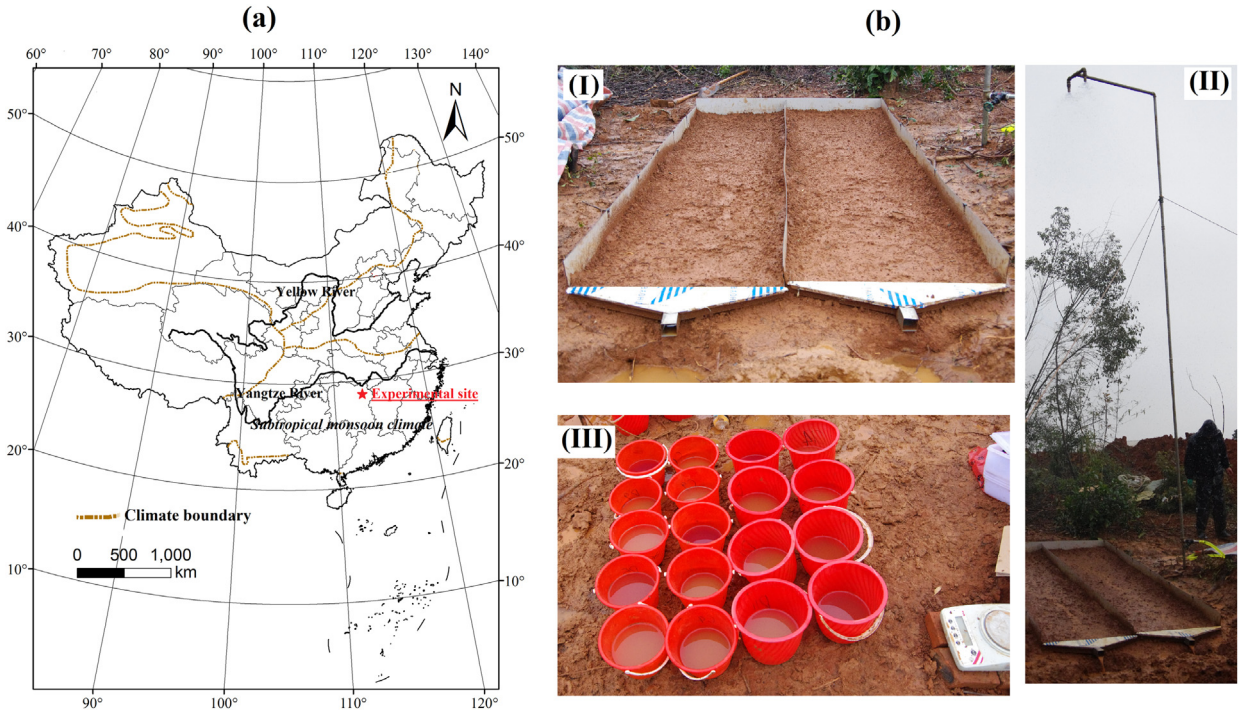

Fig. 1. Location of experimental sites (a), and field experiment components (b).

Table 1
Basic information of the selected Ultisols.

ED	Horizon	Dry color	Land use	Soil structure	Soil description
E0	A	7.5YR 6/6	forest land	granular, loose-well aggregated	high organic matter content and biological activity with a large amount of roots and plant residues
E1	B1	7.5YR 6/6	grassland	tight blocky structure	high contents of iron-manganese cutans and concretions; large amount of roots and plant residues
E2	B2		wasteland		without root and biological activity
E3	C	7.5YR6/8–5YR 4/6	bare land	tight-massive clod structure	red-white reticulated mottling horizon and heavy texture

Note: ED, erosion degree; E0, E1, E2 and E3 denote no, moderate, severe and very severe erosion degrees, respectively.

Table 2
Soil physicochemical properties in different erosion degrees (mean ± standard deviation).

ED	ρ	SOC (%)	γ (g/cm^3)	w_o (g/g)	NP (cm^3/cm^3)	CP	Sand (%)	Silt	Clay	MWD_{FM} (mm)
E0	2.70 ± 0.00	2.59 ± 0.01	1.13 ± 0.06	0.34 ± 0.03	0.16 ± 0.03	0.43 ± 0.02	7 ± 1	42 ± 1	51 ± 0	2.80 ± 0.34
E1	2.72 ± 0.01	0.28 ± 0.01	1.31 ± 0.02	0.30 ± 0.01	0.10 ± 0.02	0.42 ± 0.01	5 ± 0	44 ± 0	52 ± 0	3.50 ± 0.39
E2	2.73 ± 0.01	0.18 ± 0.02	1.31 ± 0.02	0.30 ± 0.00	0.09 ± 0.01	0.42 ± 0.01	5 ± 0	42 ± 0	53 ± 0	2.60 ± 0.14
E3	2.74 ± 0.01	0.06 ± 0.00	1.56 ± 0.01	0.23 ± 0.01	0.05 ± 0.02	0.38 ± 0.01	6 ± 0	39 ± 3	55 ± 3	4.43 ± 0.51

Note: ED, erosion degree; E0, E1, E2 and E3 denote no, moderate, severe and very severe erosion degrees, respectively; ρ, particle density; SOC, soil organic carbon; γ, bulk density; w_o, field moisture content; NP and CP, non-capillary and capillary porosity; Sand, 2–0.05 mm; Silt, 0.05–0.002 mm; Clay, < 0.002 mm; MWD_{FM}, mean weight diameter of aggregates at the field moisture content.

2.3. Data analysis

Statistical tests and figures were performed using the software of SPSS 20.0 (SPSS Inc, Chicago, IL, USA) and OriginPro 2016, respectively. The differences in soil infiltration among different treatments (erosion degree, and rainfall intensity) were analyzed at $p < 0.05$. Shapiro-Wilk statistics were conducted for the normality tests of all dependent and independent variables. Normality tests were carried out for all dependent and independent variables using Shapiro–Wilk statistics. The variables not conforming to normal distribution were transformed by natural logarithmic treatment. Soil properties accounting for the majority of soil infiltration responses were selected by stepwise multiple linear regression analysis (Xue, 2013).

3. Results

3.1. Rainfall infiltration process

The temporal variations in rainfall infiltration rate for Ultisols under different erosion degrees and rainfall intensities were depicted in Fig. 2. Time to incipient runoff (T_r) was evidently larger at the low (8.68–15.13 min) than at the high rainfall intensity (0.78–6.84 min),

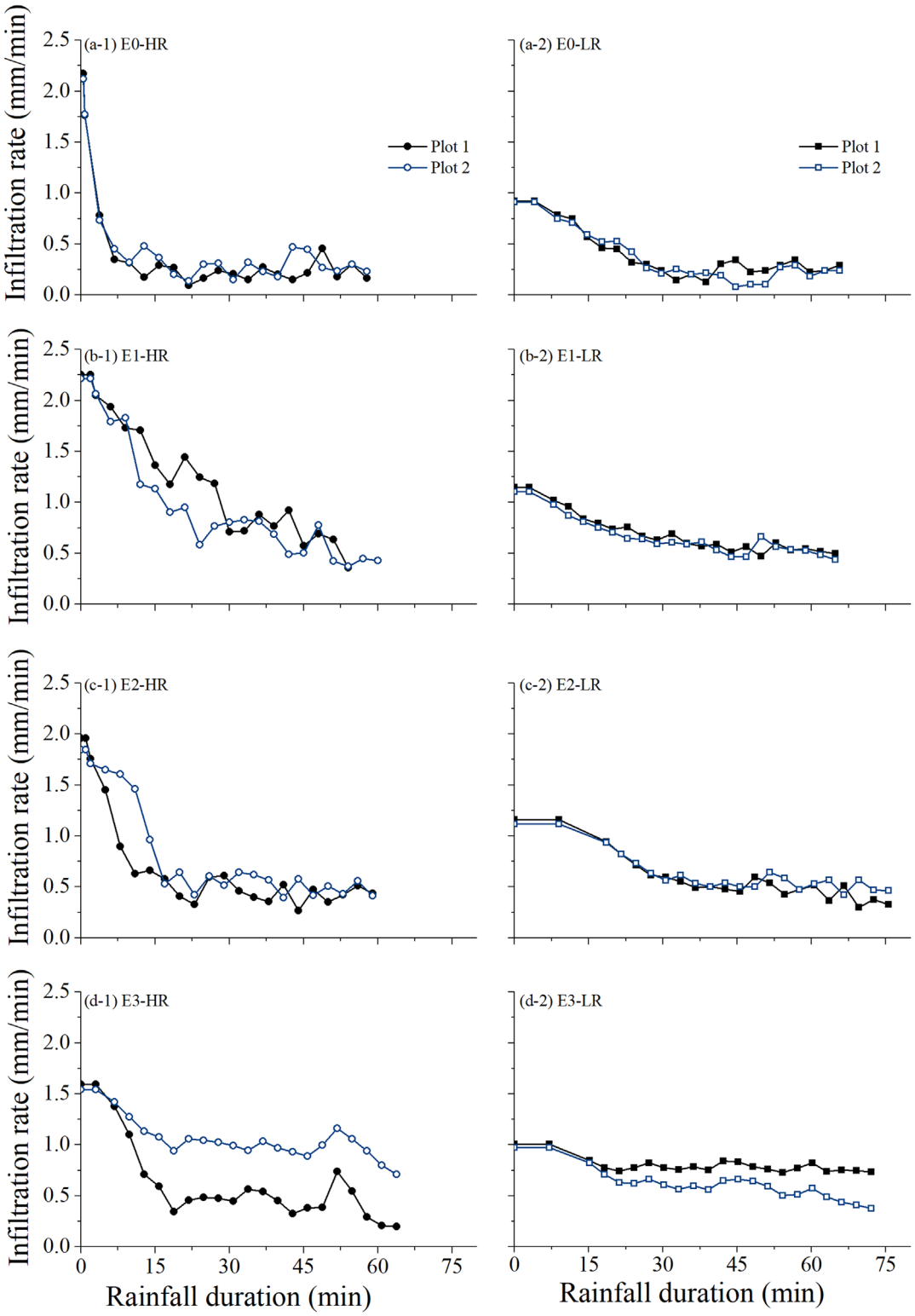

Fig. 2. Temporal variations of soil infiltration rate in different erosion classes (no (E1), moderate (E2) and very-severe (E3)) and at two rainfall intensities (60 mm/h (LR) and 120 mm/h (HR)).

and Tr at the low was around 11 times of that at the high rainfall intensity for noneroded soils (E0) (Fig. 4-a). Additionally, time to incipient runoff generally increased with the increased erosion severity especially at the high rainfall intensity. The difference of Tr between two filed plots seems to be increased with erosion severity, despite the non-eroded soils. Statistically, time to incipient runoff varied significantly with soil erosion degree and rainfall intensity ($p < 0.01$).

After runoff generation, soil infiltration rate decreased sharply after runoff generation, followed by a steady state with continuing rainfall duration. However, infiltration rate at the steady state showed apparent fluctuations, particular for soils at the high rainfall intensity. The temporal variations of infiltration rate were generally gentler at the low than at the high rainfall intensity. Similarly, the difference of temporal rainfall infiltration rate in two

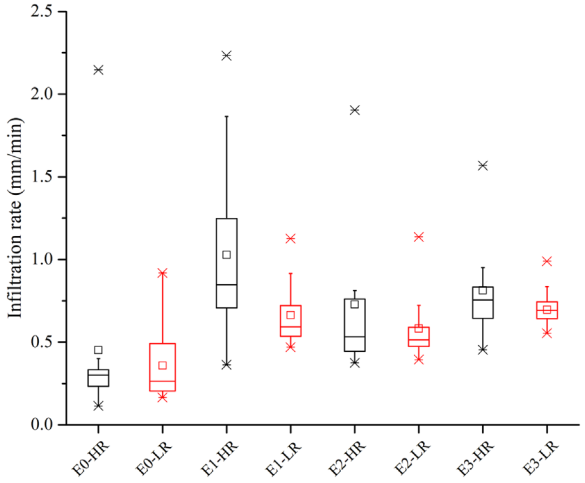

Fig. 3. Boxplots of soil infiltration rate during the rainfall for different types of soils. HR, high rainfall intensity (120 mm/h); LR, low rainfall intensity (60 mm/h); E0 = no erosion; E1 = moderate erosion; E2 = very severe erosion; E3 = very severe erosion. The boxes indicate the 25th and 75th percentiles; the line in the box indicates the median (50th percentile); "×" indicates outlier values; "□" indicates average value.

field plots was evidently larger for soils with the very severe erosion degree (E3).

The effect of erosion severity on the temporal infiltration rate varied with rainfall intensity (Fig. 3). The rainfall infiltration rate showed a relatively larger variability at the high than at the low rainfall intensity, e. g., infiltration rate of the non-eroded soils (E0) at the high and low rainfall intensity was 2.03 and 0.75 mm/min, respectively. Besides, at the high rainfall intensity, the variability of rainfall infiltration rate generally increased with increasing erosion severity, but an opposite trend was observed at the low rainfall intensity. Throughout the rainfall duration, the non-eroded soils (E0) possessed a relatively lower infiltration rate among all the tested soils, especially at the low rainfall intensity.

Infiltration process for most soil types was fitted well with Horton's equation (Adj-R^2 > 0.60, $p < 0.05$), and less satisfied fitting results were observed for the very sever eroded soils. As shown in Fig. 4-b, the decay coefficient *k* ranged between 0.03 and 1.17 for all the tested soils. Apart from the very severely eroded soils (E3), decay coefficient was generally larger at the high than at the low rainfall intensity. However, the difference of decay coefficient between two parallel field plots was significant larger at the low than at the high rainfall intensity, especially for the very severely eroded soils (1.17–0.01). Collectively, the impact of land degradation on the unsteady infiltration process varied with rainfall intensity.

The infiltration rate at the steady state averagely increased with increasing erosion severity, especially for field plot 1 at the high rainfall intensity and field plot 2 at the low rainfall intensity (Fig. 4-c). The difference of the steady state infiltration rate between the parallel treatments was obviously larger at the low rainfall intensity, besides, the infiltration rate at the steady state showed the maximum and minimum variability at field plots with moderate (E1) and very sever (E3) erosion degree, respectively.

3.2. Identification of soil properties influencing rainfall infiltration processes

Multiple stepwise regression results (Fig. 5) indicated that rainfall infiltration process of Ultisols was significantly influenced by rainfall intensity, mean weight diameter of aggregates at the field moisture content, soil organic carbon and particle size distribution ($p < 0.05$). Specifically, rainfall intensity and clay content

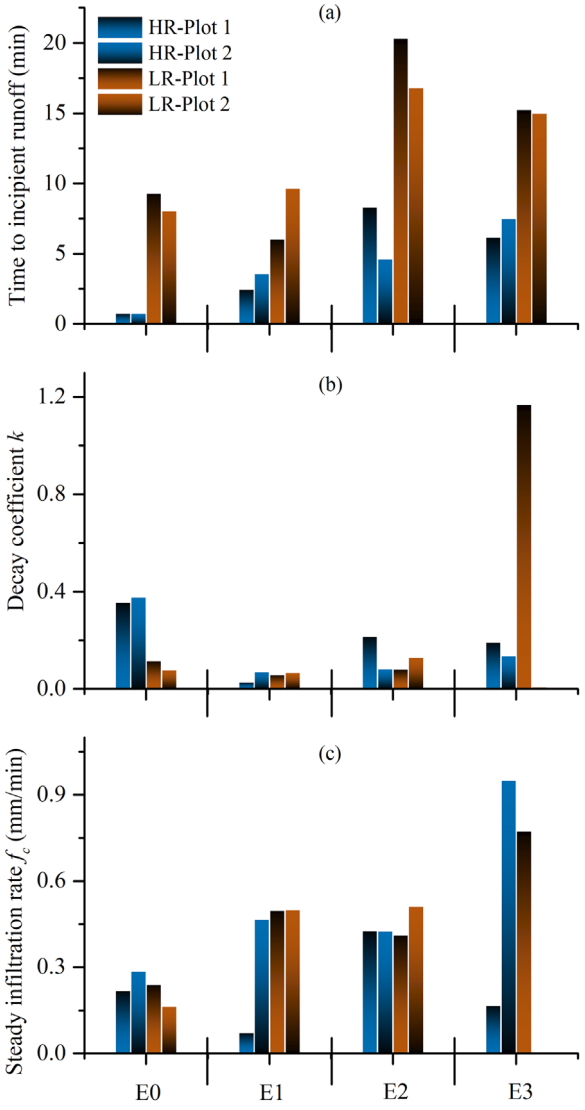

Fig. 4. Parameters of Horton models including (a) Time to incipient runoff (T_r), (b) decay coefficient *k* and (c) steady state infiltration rate (f_c) in different erosion classes (no (E1), moderate (E2) and very-severe (E3)) and at two rainfall intensities (60 mm/h (LR) and 120 mm/h (HR)).

with negative and positive effects on time to incipient runoff (Tr), respectively, explained more than 80% of variance in Tr (Adj-R^2 = 75%, $p < 0.05$). However, the variability of the time to incipient runoff was largely depended on the sand content ($p < 0.01$). The decay coefficient (*k*) with its variability determined by clay content (R^2 = 75%, $p < 0.01$) was decreased by the increasing silt content (R^2 = 56%, $p < 0.01$). The content of soil organic carbon and clay fraction contributed to variation of the infiltration rate at the steady state (f_c) (Adj-R^2 = 79%, $p < 0.01$), besides, the variability of f_c was influenced by mean weight diameter of aggregates at the field moisture content (R^2 = 82%, $p < 0.01$). Generally, the final infiltration rate was determined by soil cement content and aggregate stability.

Considering the significant effects of rainfall intensity on soil infiltration rate, the relationships between rainfall infiltration processes and the influencing factors were analyzed separately under different rainfall intensities (Fig. 5-b and -c). At the high rainfall intensity, clay content facilitated the increasing of the time to incipient runoff (R^2 = 72%, $p < 0.01$) with its variability increased by the interaction of sand content and aggregate stability index (Adj-R^2 = 81%, $p < 0.05$); the variation of decay coefficient

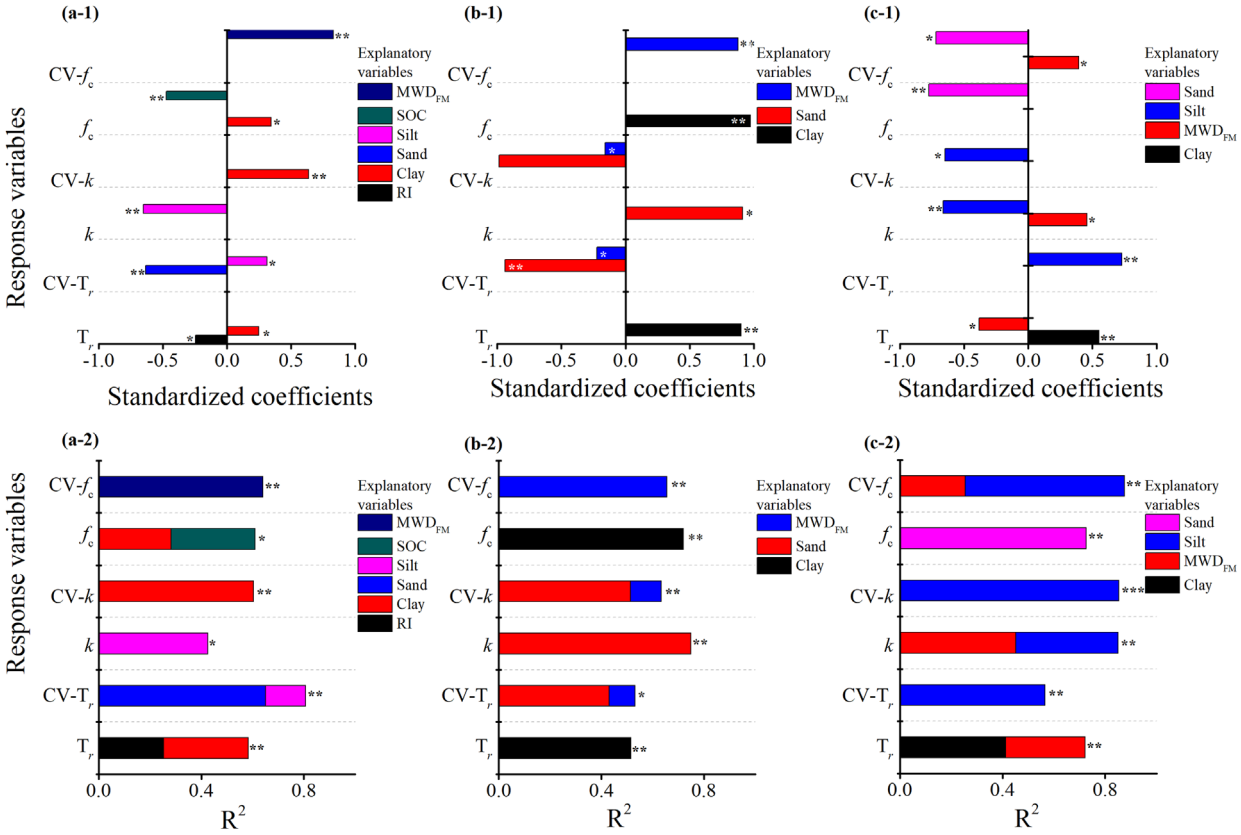

Fig. 5. Standardized coefficients and R square of selected variables accounting for the Horton model parameters based on the all data (a), at the high rainfall intensity (b) and at the low rainfall intensity (c).

(k) was dominated by sand content ($R^2 = 0.62\%$, $p < 0.001$); clay content ($R^2 = 0.82\%$, $p < 0.01$) and mean weight diameter of aggregates at the field moisture level ($R^2 = 0.79\%$, $p < 0.01$) generated the variation and variability of the steady state infiltration rate, respectively. At the low rainfall intensity, time to incipient runoff was influenced by the interaction of clay content and mean weight diameter of aggregates at the field moisture level (Adj-$R^2 = 81\%$, $p < 0.05$), but its variability was generated by silt content ($R^2 = 0.79\%$, $p < 0.01$); silt content ($R^2 = 52\%$, $p < 0.01$) and the mean weight diameter of aggregates at the field moisture level ($R^2 = 0.38\%$, $p < 0.05$) was negatively and positively correlated with the decay coefficient (k), respectively; the variation of steady state infiltration rate was determined by sand content ($R^2 = 83\%$, $p < 0.01$). Collectively, clay and sand content dominated the major variation of rainfall infiltration process at the high rainfall intensity, but silt content contributed to the variation of rainfall infiltration process at the low rainfall intensity.

4. Discussion

According to this study, the variation rainfall infiltration rate was generally changed into three parts: (i) keeping constantly before runoff generation; (ii) declining sharply with rainfall duration; (iii) obtaining a steady state finally. The rainfall infiltration process for bare soils was predominated by the variation of surface soil properties and structures (Assouline, 2004; Carmi & Berliner, 2008), which was intrinsically determined by the extent of the breakdown and dispersion of soil aggregates under the interacts of rainfall (intensity and duration) and surface structure stability (Ran, Su, Li, & He, 2012). Ultisols suffering from different land degradation degrees showed different infiltration processes, altering the sediment transportability and concentration, and hence, influencing the erosion process.

4.1. Effects of rainfall characteristics on rainfall infiltration process

During rainfall, the temporal infiltration process could be reduced by the formation and evolution of surface crusts (Carmi & Berliner, 2008; Ran, Su, Li, & He, 2012). At the initial stage of rainfall, soils possessed a high infiltration capacity, delaying the time to incipient runoff; as rainfall continued, surface structure was gradually compacted by the raindrop impact, especially at the high rainfall intensity and high kinetic energy, and thus facilitated the runoff generation but declined the infiltration (Shi, Yan, Li, Li, & Cai, 2010), as the variation of time to incipient runoff showed in Fig. 4-a. Simultaneously, high rainfall intensity usually contributed to the breakdown of more aggregates and facilitated surface crust formation and pore clogging (Lu, Zheng, Li, Bian, & An, 2016) (Fig. S3), which could also explain the negative effects of rainfall intensity on runoff generation (Fig. 5-a) and the decreased infiltration rate with rainfall duration (Fig. 2).

Surface crusting was formed by an in situ reorganization of existing aggregates and dispersive fragments or sedimentary crusts generated by particle transport and sorting (Le Bissonnais et al., 2005). However, this process was influenced by the dual contribution of rainfall intensity. High rainfall intensity disrupted more soil aggregates (except the very severely eroded soils), facilitating the formation of surface crusts but it also possessed a high sediment transport capacity. Therefore, different degrees of surface crust formation during the continued rainfall duration generated the various infiltration patterns in Fig. 2. Specifically, the well-developed crusting leaded to a nearly constant infiltration rate at the steady state, e.g., the quasi-steady state of infiltration

rate of non-eroded soils (Fig. 2-a). Yet, the re-disrupted crust could be transported by runoff, particular under the high runoff coefficient condition (Fig. S4). The transportability of runoff and the detachment ability of rain drops collectively affected the variation of surface structure and infiltration fluctuation.

4.2. Effects of soil properties on rainfall infiltration process

The variation of surface structure or crusting generated by the mechanical breakdown and dispersion of aggregates for the pre-wetted soils under the rainfall condition (Le Bissonnais, 1996; Shi, Yan, Li, Li, & Cai, 2010). Apart from the rainfall intensity, soil properties and surface soil conditions also made great contributions to the dynamic infiltration rate during rainfall events (Assouline & Ben-Hur, 2006). Due to the different disruptive forces of rainfall intensities, different soil properties were selected to account for the temporal infiltration rate at the high and low rainfall intensity (Fig. 5). During rainfall, sediment transport by runoff dominated the surface variation, indicated by particle size distribution (Kinnell, 2005). This was supposed to be the reason that the content of clay, silt and sand fraction contributed to the variation of infiltration process for Ultisols. Besides, the loos structure (bulk density was in a range of 1.13–1.31 g/cm^3) (Table 2) of the non-eroded (E0), moderately eroded (E1), and severely eroded soils (E2) soils facilitated the disintegration of soil particles and the formation of structural crust (Le Bissonnais, 1996), and hence, the tight density and low permeability of these crusts generated the sharp decreasing of infiltration rate especially at high rainfall intensity (Fig. 2-a–c). Likewise, the relative tight-blocky structure (bulk density was around 1.56 g/cm^3) and high mechanical strength (mean weight diameter of aggregates at the field moisture content was around 4.43 mm) of the very severely eroded soils (E3), accelerated its resistance to rainfall impact and runoff dispersion, resulting in a less susceptibility to breakdown (Misra & Teixeira, 2001), which leaded to a relatively high infiltration rate and less influence by rainfall duration (Fig. 2d). In addition, the rough surface for the very severely eroded soils would reduce the detachment power and transport capacity of runoff, thus enabling a higher infiltration (Prosdocimi et al., 2017).

4.3. Variation of soil loss influenced by erosion degree and rainfall intensity

The hydrological process during rainfall is composed by infiltration and runoff, and the increased runoff or decreased infiltration contributes to increasing the sediment concentration (e.g., Jin et al., 2008; Tadesse, Suryabhagavan, Sridhar, & Legesse, 2017). Though, most of the obtained results in this study were consistent with this conclusion, the effect of infiltration on sediment concentration varied with erosion degree and rainfall intensity (Fig. S5) (Fig. 6), e.g., sediment concentration was positively correlated with infiltration rate for non (E0) and moderately (E1) eroded soils at the high rainfall intensity, and for the very severely eroded soils (E3) at the high and low rainfall intensity ($p < 0.05$). The positive and non-significant correlations could be ascribed by the variation of sediment transport form during erosion process (Assouline & Ben-Hur, 2006; Kinnell, 2005; Mohamadi & Kavian, 2015). It was speculated that soil loss was predominated by detachment-limited regime for the very severely eroded soils (E3) and transport-limited form for the non (E0) and moderately (E1) eroded soils at the high rainfall intensity (Kukal & Bawa, 2013).

In eroded inferior lands, soil was exposed to erosion once losing the surface cover (Kirchhoff, Rodrigo-Comino, Seeger, & Ries, 2017). Surface crusts formed during rainfall induced erosion made dual effects on soil loss: (1) impeding a further detachment of raindrop and runoff to subsurface aggregate, which reduced infiltration and soil loss; (2) increasing the amount of runoff, which momentarily improved the ability of detachment and transport for overland flow. Widely accepted that, surface crusts facilitate particles compaction and clog soil pores, leading to a much lower permeability of the crusted surface than that of the underlying layers (Assouline, 2004), but crust formation reduces the infiltration rate, which increases runoff and accelerates the soil loss (Durán Zuazo & Rodríguez Pleguezuelo, 2008). However, in this

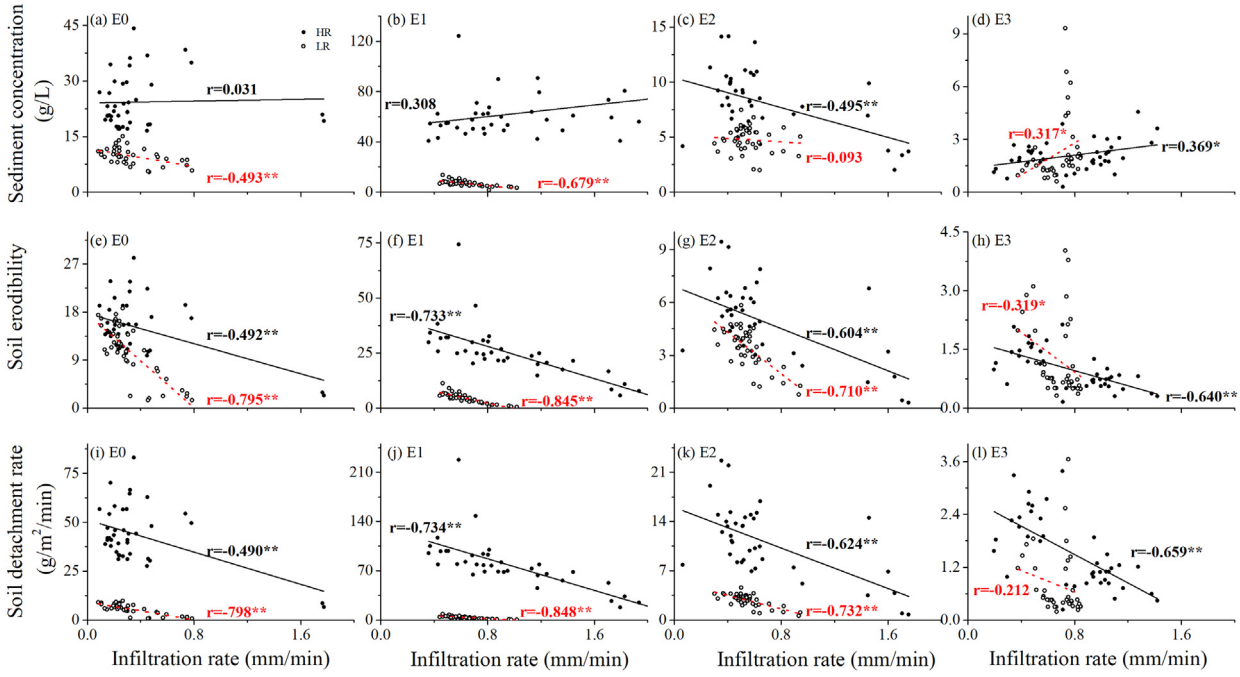

Fig. 6. Relationships of sediment concentration, soil erodibility, and soil detachment rate with infiltration rate. HR and LR indicate high (120 mm/h) and low (60 mm/h) rainfall intensity, respectively. * and ** represent the statistical significance at $p < 0.05$, and 0.01, respectively. The relationship in each treatment was derived from the two plot data rather than their average value ($n = 40$).

study, a significant and negative correlation ($p < 0.01$) has been observed between the temporal soil erodibility and infiltration rate for all the tested soils (Fig. 6). It is noteworthy that, this positive correlation actually reflected the temporal influence of surface crusting to soil erodibility. Surface crusting with high mechanical strength could increase surface shear strength and improve the anti-erodibility of surface soil temporally, compared with the original loss and well aggregated surface structure (Kinnell, 2006; Wei, Wu, & Cai, 2015).

Similar correlation was observed between soil detachment rate and infiltration rate ($r < 0$, $p < 0.01$). The correlation was higher at the low ($r = -0.73$ to -0.89, $p < 0.01$) than at the high rainfall intensity ($r = -0.49$ to -0.73) except for the very severely eroded soils (E3) showing and opposite trend, indicating that soil loess was determined by the transport capacity of runoff, especially at the low rainfall intensity for E0, E1 and E2. Besides, the increased runoff would facilitate the breakdown of the thin crust and then percolated through the subsurface soils, which likely leaded to the fluctuation of rainwater partitioning in the steady state and accelerated erosion on subsurface soils (Ribolzi et al., 2011). Therefore, topsoil was crucial for soil erosion induced by rainfall. Increasing surface cover (such as vegetation and mulch) should be an imperative way to inhibit the formation of soil crust and improve the crop water availability especially for soils in a well aggregate and loose structure (Dlamini et al., 2011; Tadesse, Suryabhagavan, Sridhar, & Legesse, 2017). However, the very severely eroded soils with high infiltration capacity were less productive due to the deficiency of essential elements and structure conditions for crop growth, and hence, different measurements should be considered in practice.

5. Conclusions

In this study, the effects of erosion induced land degradation and rainfall intensity on infiltration process in the Ultisols was investigated by the field plot rainfall simulation experiments. Soil infiltration processes, including time to incipient runoff, the decay coefficient and the steady state infiltration rate, and their variability were generally larger at the high than at the low rainfall intensity, and showed an increasing trend with the increased erosion severity. The dynamic infiltration rate was dominated by rainfall intensity, mean weight diameter of aggregates at the field moisture content, soil organic carbon and particle size distribution, and the specific physicochemical properties that controlling the hydraulic process varied with rainfall intensity. Increasing surface cover should be considered for inhibiting soil erosion for soils with well aggregate and loose structure; but the improvement of soil fertility and structure for the very severely eroded soils is more imperative. The results of this study were obtained based on the hypothesis that soil infiltration differs significantly between land degradation levels and rainfall intensities, and other factors for the field rainfall simulation experiments including slope, bare fallow condition, and antecedent moisture condition of experiment plots kept as consistent as possible. Despite these factors, the hydrological response under the dynamic rainfall intensity also need a further investigation in future studies.

Acknowledgements

This research was supported by the National Key Research and Development Program of China (2017YFC0505401) and the National Natural Science Foundation of China (41807065).

Appendix A. Supplementary material

Supplementary data associated with this article can be found in the online version at https://doi.org/10.1016/j.iswcr.2018.12.005.

References

Assouline, S. (2004). Rainfall-induced soil surface sealing: A critical review of observations, conceptual models, and solutions. *Vadose Zone Journal*, *3*, 570–591.
Abudi, I., Carmi, G., & Berliner, P. (2012). Rainfall simulator for field runoff studies. *Journal of Hydrology*, *454–455*, 76–81.
Almeida, W. S. D., Panachuki, E., Oliveira, P. T. S. D., Menezes, R. D. S., Sobrinho, T. A., & Carvalho, D. F. D. (2018). Effect of soil tillage and vegetal cover on soil water infiltration. *Soil & Tillage Research*, *175*, 130–138.
Assouline, S., & Ben-Hur, M. (2006). Effects of rainfall intensity and slope gradient on the dynamics of the interrill erosion during soil surface sealing. *Catena*, *66*, 211–220.
Bossio, D., Geheb, K., & Critchley, W. (2010). Managing water by managing land: Addressing land degradation to improve water productivity and rural livelihoods. *Agricultural Water Management*, *97*, 536–542.
Bhan, S. (2013). Land degradation and integrated watershed management in India. *International Soil and Water Conservation Research*, *1*(1), 49–57.
Cerdà, A. (1999). Seasonal and spatial variations in filtration rates in badland surfaces under Mediterranean climatic conditions. *Water Resources Research*, *35*(1), 319–328.
Carmi, G., & Berliner, P. (2008). The effect of soil crust on the generation of runoff on small plots in an arid environment. *Catena*, *74*, 37–42.
Durán Zuazo, V. H., & Rodríguez Pleguezuelo, C. R. (2008). Soil-erosion and runoff prevention by plant covers. A review. *Agronomy for Sustainable Development*, *28*, 65–86.
Dlamini, P., Orchard, C., Jewitt, G., Lorentz, S., Titshall, L., & Chaplot, V. (2011). Controlling factors of sheet erosion under degraded grasslands in the sloping lands of KwaZuluNatal. *South Africa Agricultural Water Management*, *98*, 1711–1718.
Gao, Y. X., Li, J., & Zhou, M. C. (1998). *Soil map of China (1:4,000,000)* (pp. 1–6) Beijing: Since Press (In Chinese).
García-Ruiz, J. M., Beguería, S., Lana-Renault, N., Nadal-Romero, E., & Cerdà, A. (2017). Ongoing and emerging questions in water erosion studies. *Land Degradation & Development*, *28*, 5–21.
Gonzalez, J. M. (2018). Runoff and losses of nutrients and herbicides under long-term conservation practices (no-till and crop rotation) in the U.S. Midwest: A variable intensity simulated rainfall approach. *International Soil and Water Conservation Research*, *6*, 265–274.
Horton, R. E. (1941). An approach toward a physical interpretation of infiltration-capacity 1. *Soil Science Society of America Journal*, *5*(C), 399–417.
Huang, J., Wu, P., & Zhao, X. (2013). Effects of rainfall intensity, underlying surface and slope gradient on soil infiltration under simulated rainfall experiments. *Catena*, *104*, 93–102.
Jin, K., Cornelis, W. M., Gabriels, D., Shiettecatte, W., Neve, S. D., Lu, J., & Harmann, R. (2008). Soil management effects on runoff and soil loss from field rainfall simulation. *Catena*, *75*, 191–199.
Kinnell, P. I. A. (2005). Raindrop impact induced erosion processes and prediction: A review. *Hydrological Processes*, *19*, 2815–2844.
Kinnell, P. I. A. (2006). Simulations demonstrating interaction between coarse and fine sediment loads in rain-impacted flow. *Earth Surface Processes and Landforms*, *31*, 355–367.
Kukal, S. S., & Bawa, S. S. (2013). Temporal variations in runoff and soil loss in relation to soil conservation practices in catchments in Shiwaliks of lower Himalayas. *International Soil and Water Conservation Research*, *1*(2), 19–25.
Kirchhoff, M., Rodrigo-Comino, J., Seeger, M., & Ries, J. B. (2017). Soil erosion in sloping vineyards under conventional and organic land use managements (Saar-Mosel Valley, Germany). *Cuadernos Délelőtt Investigación Geográfica*, *43*.
Luk, S., Abrahams, A. D., & Parsons, A. J. (1986). A simple rainfall simulator and trickle system for hydro-geomorphic experiments. *Physical Geography*, *7*(4), 344–356.
Le Bissonnais, Y. (1996). Aggregate stability and assessment of soil crustibility: I. Theory and methodology. *European Journal of Soil Science*, *47*, 425–437.
Lal, R. (2001). Soil degradation by erosion. *Land Degradation & Development*, *12*, 519–539.
Le Bissonnais, Y., Cerdan, O., Lecomte, V., Benkhadra, H., Souchère, V., & Martin, P. (2005). Variability of soil surface characteristics influencing runoff and interrill erosion. *Catena*, *62*, 111–124.
Liu, H., Lei, T. W., Zhao, J., Yuan, C. P., et al. (2011). Effects of rainfall intensity and antecedent soil water content on soil infiltrability under rainfall conditions using the run off-on-out method. *Journal of Hydrology*, *396*, 24–32.
Lu, J., Zheng, F., Li, G., Bian, F., & An, J. (2016). The effects of raindrop impact and runoff detachment on hillslope soil erosion and soil aggregate loss in the Mollisol region of Northeast China. *Soil & Tillage Research*, *161*, 79–85.
Misra, R. K., & Teixeira, P. C. (2001). The sensitivity of erosion and erodibility of forest of soils to structure and strength. *Soil & Tillage Research*, *59*, 81–93.
Malvar, M. C., Martins, M. A., Nunes, J. P., Robichaud, P. R., & Keizer, J. J. (2013). Assessing the role of pre-fire ground preparation operations and soil water

repellency in post-fire runoff and inter-rill erosion by repeated rainfall simulation experiments in Portuguese eucalypt plantations. *Catena*, *108*, 69–83.
Mohamadi, M. A., & Kavian, A. (2015). Effects of rainfall patterns on runoff and soil erosion in field plots. *International Soil and Water Conservation Research*, *3*(4), 273–281.
Morbidelli, R., Saltalippi, C., Flammini, A., & Govindaraju, R. S. (2018). Role of slope on infiltration: A review. *Journal of Hydrology*, *557*, 878–886.
Podwojewski, P., Janeau, J. L., Grellier, S., Valentin, C., Lorentz, S., & Chaplot, V. (2011). Influence of grass soil cover on water runoff and soil detachment under rainfall simulation in a sub-humid South African degraded rangeland. *Earth Surface Processes and Landforms*, *36*, 911–922.
Prosdocimi, M., Burguer, M., Di Prima, S., Sofia, G., Terol, E., Rodrigo Comino, J., … Tarolli, P. (2017). Rainfall simulation and structure-from-motion photogrammetry for the analysis of soil water erosion in Mediterranean vineyards. *Science of the Total Environment*, *574*, 204–215.
Rejman, J., Turski, R., & Paluszek, J. (1998). Spatial and temporal variations in erodibility of loess soil. *Soil & Tillage Research*, *46*, 61–68.
Ribolzi, O., Patin, J., Bresson, L. M., Latsachack, K. O., Mouche, E., Sengtaheuanghoung, O., & Valentin, C. (2011). Impact of slope gradient on soil surface features and infiltration on steep slopes in northern Laos. *Geomorphology*, *127*, 53–63.
Ran, Q., Su, D., Li, P., & He, Z. (2012). Experimental study of the impact of rainfall characteristics on runoff generation and soil erosion. *Journal of Hydrology*, *424*, 99–111.
Rodrigo Comino, J., Iserloh, T., Lassu, T., Cerdà, A., Keestra, S. D., Prosdocimi, M., … Ries, J. B. (2016). Quantitative comparison of initial soil erosion processes and runoff generation in Spanish and German vineyards. *Science of the Total Environment*, *565*, 1165–1174.
Shakesby, R. A., Doerr, S. H., & Walsh, R. P. D. (2000). The erosional impact of soil hydrophobicity: Current problems and future research directions. *Journal of Hydrology*, *231–232*, 178–191.
Shi, Z. H., Yan, F. L., Li, L., Li, Z. X., & Cai, C. F. (2010). Interrill erosion from disturbed and undisturbed samples in relation to topsoil aggregate stability in red soils from subtropical China. *Catena*, *81*, 240–248.
Tadesse, L., Suryabhagavan, K. V., Sridhar, G., & Legesse, G. (2017). Land use and land cover changes and Soil erosion in Yezat Watershed, North Western Ethiopia. *International Soil and Water Conservation Research*, *5*(2), 85–94.
Walker, J. D., Walter, M. D., & Parlange, J. Y. (2007). Reduced raindrop-impact driven soil erosion by infiltration. *Journal of Hydrology*, *342*, 331–335.
Wei, Y., Wu, X., & Cai, C. (2015). Splash erosion of clay-sand mixtures and its relationship with soil physical properties: The effects of particle size distribution on soil structure. *Catena*, *135*, 254–262.
Wu, X., Cai, C., Wang, J., Wei, Y., & Wang, S. (2016). Spatial variations of aggregate stability in relation to sesquioxides for zonal soils, South-central China. *Soil & Tillage Research*, *157*, 11–22.
Xue, W. (2013). *SPSS statistical methods and applications* ((3th ed.). Beijing, China: Publishing House of Electronics Industry (in Chinese).
Zhang, B., Yang, Y., & Zepp, H. (2004). Effect of vegetation restoration on soil and water erosion and nutrient losses of a severely eroded clayey Plinthudult in southeastern China. *Catena*, *57*, 77–90.